

Shear behaviors of precast concrete wall panel structures with top connecting reinforcements of CFRP bars in vertical joints

S. Mochizuki
 Musashi Institute of Technology, Tokyo, Japan

ABSTRACT: In joints of precast concrete wall panel structures, in-plane restrictions are known to be effective to shear strength. Among in-plane restrictions of vertical joints, the most importance is the restriction by top connecting reinforcements of wall panels. The restriction is considered to be affected by the tensile rigidity as well as the tensile strength of top connecting reinforcements. This paper concerns the experimental study on effects by the rigidity and the strength of top connecting reinforcements to shear strength of vertical joints of wall panel structures. Results presented in this paper give the materials to establish the design method of vertical joints controlling the failure modes of wall panel structures.

1. Introduction

At one of the new construction methods of precast concrete wall panel, it can be proposed that cotter bars are substituted by top connecting reinforcements at the level of floor slab in the vertical joints in Japan. Under these background, there are many studies²⁾ about shear strength of vertical joints by the strength of top connecting reinforcements, but few, by rigidity of top connecting reinforcements. The object of this paper is to clarify the restrictive effects of the tensile rigidity as well as the tensile strength of top connecting reinforcements to shear strength of vertical joint and failure modes of wall panel structures.

2 TEST PROCEDURE

2.1 Specimens

Specimens are cantilever-type ones with vertical joints assembling two wall panels, 928 mm high, 400mm wide and 125mm thick each, and horizontal joints connecting wall panels with foundation girder or loading stub as shown in Fig.1.

Transverse reinforcements at vertical joint (*transverses reinforcements for abbreviation*) are through ones without joints expecting welded joints in reality. Longitudinal reinforcements at horizontal joints (*longitudinal reinforcements for abbreviation*) between wall panels and foundation girder are linked by mortar grouted into splice sleeves. To clarify the effect of tensile rigidity and strength of top connecting reinforcement

(TCR for abbreviation) to characteristics of vertical joints, carbon fiber reinforced plastic (CFRP for abbreviation) reinforcements NFM2, NFM4 are used as the TCR with different rigidity and strength. CFRP reinforcements are inserted into sleeve in range of vertical joints to avoid shear break. Summary of structural factors of two

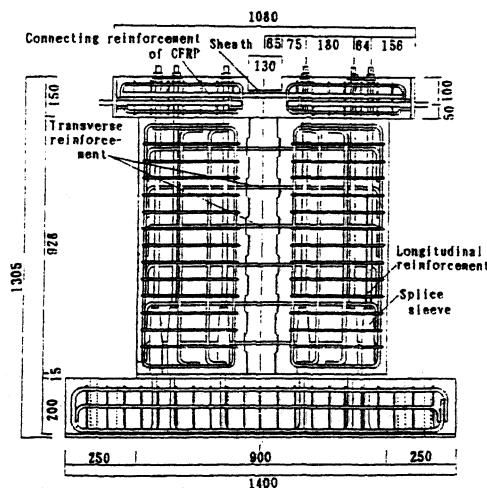


Fig.1 Configuration of Specimen (unit:mm)

Table 1 Summary of Structural Factors

Specimen	Cotter	Longitudinal Rein.		TCR	Transverse Rein.	
	Area (cm ²)	Area (cm ²)	Ratio of Longitudinal Rein. (%)	Area (cm ²)	Area (cm ²)	Ratio of Transverse Rein. (%)
WPC-N2	315.0	4.28	0.369	1.970 (2 NFM2)	11.94	1.06
WPC-N4	7.0x7.5 x6p	5-D10		3.628 (2 NFM4)	6-D16	

Table 2 Properties of Materials

CONCRETE AND MORTAR	Gasting Place	Compressive Strength (kg/cm ²)		Tensile Strength (kg/cm ²)		Yonug's Modulus (x10 ⁶ kg/cm ²)	
		WPC-N2	WPC-N4	WPC-N2	WPC-N4	WPC-N2	WPC-N4
		Foundation, Girder	360	373	22.8	26.7	2.53
Wall Panel	395	402	19.2	28.8	2.43	2.46	
Layer Mortar	100	382	—	—	2.51	2.49	
Vertical Joint	311	329	21.5	21.3	2.66	2.51	
Grout Mortar	723	723	—	—	2.91	2.91	
REINFORCEMENT AND CFRP	Reinforcement	Yield Strength (kg/cm ²)	Tensile Strength (kg/cm ²)	Young's Modulus (x10 ⁶ kg/cm ²)			
	D6, 10, 13, 16	3581~3769	5033~5578	1.30~1.68			
	CFRP	Area (cm ²)	Tensile Strength (kg/cm ²)	Young's Modulus (x10 ⁶ kg/cm ²)			
	NFM2	0.985	10540	0.92			
	NFM4	1.814	7560	1.26			

Table 3 Summary of Strengths

Specimen	Cracking Load							Maximum Strength (τ _{max})	
	Joint			Wall Panel		TCP			
	Q _{JH} (τ _{JH})	Q _{JV} (τ _{JV})	Q _{JF} (τ _{JF})	Q _{WP} (τ _{WP})	Q _{WP} (τ _{WP})	Q _{TCP}	Q _{TCP}		
WPC-N2	+	5.3 (4.7)	21.3 (18.3)	21.3 (18.3)	10.6 (8.4)	22.0 (18.6)	21.0	21.9	26.5 (22.3)
	-	5.6 (5.0)	16.1 (13.9)	20.5 (17.7)	12.2 (10.9)	22.8 (20.3)	21.5	20.5	26.3 (22.6)
WPC-N4	+	7.6 (6.8)	16.5 (14.2)	25.2 (21.3)	13.1 (11.6)	22.0 (19.5)	11.5	—	28.9 (24.9)
	-	6.7 (5.9)	19.3 (16.5)	22.0 (19.0)	16.0 (14.3)	21.3 (18.9)	—	—	28.6 (24.7)

Symbols: Q_{JH}: Cracking load along interface of horizontal joint (tf)
 Q_{JV}: Cracking load along interface of vertical joint (tf)
 Q_{JF}: Shear cracking load at vertical joint (tf)
 Q_{WP}: Flexural cracking load in wall panel (tf)
 Q_{TCP}: Shear cracking load in wall panel (tf)
 Q_{TCP}: Shear cracking load in TCP (tf)
 Q_{TCP}: Flexural cracking load in TCP (tf)
 Q_{max}: Maximum strength (tf)
 Values in () are average shear stress (kg/cm²)

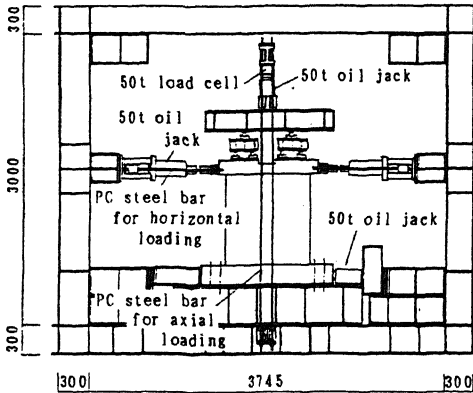


Fig. 2 Loading Equipment (unit:mm)

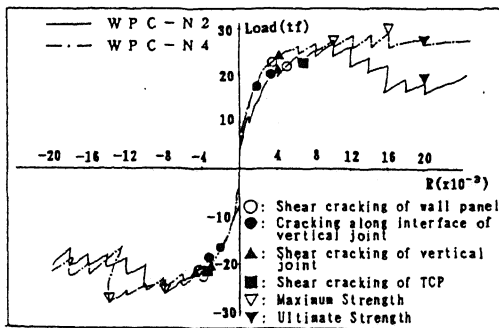


Fig. 3 Load-Rotation Angle Curves

specimens performed in the test are shown in Table 1. Table 2 shows the properties of materials used in the test.

2.2 Methods of loading and measurement

The loading equipment is shown in Fig.2. Horizontal loading is the cyclic reverse one controlled by rotation angle R (=1,2,4,6,..., 25x10⁻³rad). Horizontal loading is equal tensile and compressive loading simultaneously applied at both ends of loading stub by two oil jack. While compressive loading is applied by pushing the loading stub di-

rectly, tensile force by pulling the PC steel bars embedded into the opposite half of loading stub. This horizontal loading method is thought to be an ideal one. Axial stress is 22.0kg/cm².

Displacements are measured by sensitive displacement meters, such as horizontal and vertical displacement of wall panel as a whole and relative sliding and opening displacements between panel and panel, and between panel and foundation girder. Strain of reinforcements are measured by strain gauges sticked on transverse, longitudinal and TCR.

3 TEST RESULTS

3.1 Failure process

The load-rotation angle curves and various strength are shown in Fig.3 and Table 3, respectively. In both specimens, at first, a split crack appeared along the interface of horizontal joint. And the crack extended over the interface of the joint before rotation angle reached 1.0x10⁻³rad. When rotation angle was 4.0~6.0x10⁻³rad, transverse flexural cracks appeared near the center of wall panel. Towards the same time, the longitudinal split cracks along the interface and shear cracks of joint concrete of vertical joint appeared nearly simultaneously, and they connected immediately. Afterward, for WPC-N2 sliding and opening displacements between wall panel and joint concrete developed and concrete failure along cotter interface was observed. While shear cracks at top connecting part (TCP for abbreviation) occurred when rotation angle was 6.4x10⁻³rad. for WPC-N2, flexural cracks only, for WPC-N4. Maximum strengths of WPC-N2, WPC-N4 were 26.5tf, 28.6tf respectively. Sudden fall of strength was accompanied with the maximum strength for WPC-N2 and strength decreased to 20.0tf when rotation angle was 20.0x10⁻³rad. After that, the specimen behaved without ductility. On the other hand, WPC-N4 showed ductil characteristic without fall of strength until the ultimate at positive loading, though temporary fall of strength due to cracks of layer mortar at

negative loading occurred.

3.2 Strain and displacement

The distribution of longitudinal reinforcements at positive loading are shown in Fig. 4. As known from Fig. 4 neutral axis for both specimens predicted from the strain of longitudinal reinforcements located in the vicinity of vertical joint before 2.0×10^{-3} rad. After the shear crack was observed at the vertical joint, while WPC-N2 shows the distribution as two isolated wall panels, WPC-N4 shows as a united wall panel. Relative sliding between wall panels are shown in Fig. 5. In relative sliding displacements measured at the top, center and bottom of panel in Fig. 5, great difference between WPC-N2 and WPC-N4 is observed in the absolute quantity. The relative sliding displacements for WPC-N4 using NFM4 of high Young's modulus are less than those for WPC-N2. The increase of the relative sliding displacements for WPC-N2 is due to weak restraint by elongation of NFM2 of low Young's modulus. Fig. 6 shows the relations between the average axial bearing force obtained from strain values of TCR and rotation angles. The tendency of increase of the axial bearing force continued until rotation angle of 8.0×10^{-3} rad. The axial bearing force maintained constant values after that for WPC-N4. On the other hand, the axial bearing force continued to increase after the maximum strength at rotation angle of 10×10^{-3} rad, for WPC-N2 to avoid the separation between two wall panels by the restraint of TCR.

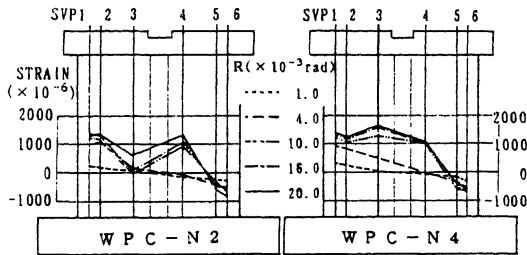


Fig. 4 Strain Distribution of Longitudinal Reinforcements

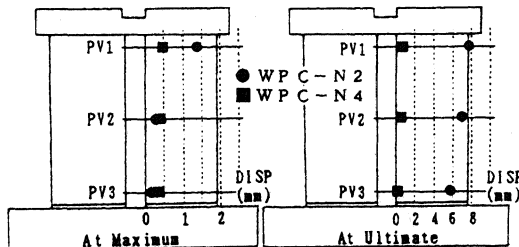


Fig. 5 Relative Sliding Displacement between Wall Panels

4 MAXIMUM AND ULTIMATE STRENGTH

Fig. 7 shows models of resistant mechanisms of a united wall panel type and two isolated one. In case of which the maximum strength is controlled by flexural yielding, the ultimate strength is equal to the maximum one. In case of which the maximum strength is controlled by shear failure of vertical joint, the ultimate strength is sum of each flexural strength of two isolated wall panels. From the experimental results, while the maximum strength is resulted from shear failure of vertical joint for WPC-N2, the maximum for WPC-N4, flexural yielding of a

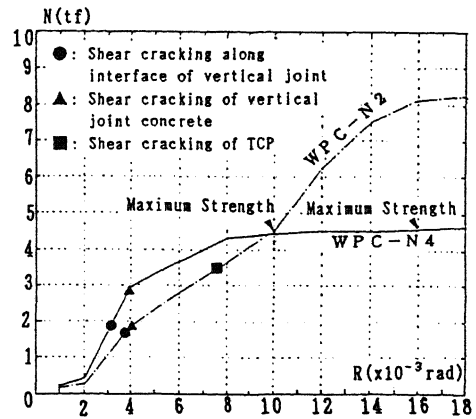


Fig. 6 Relations between Axial Bearing Forces of TCR and Rotation Angle

united wall panel. From the past S-type shear experiment by the author in which NFM was used as joint reinforcements, effective ratio CN of axial bearing forces at the maximum and the ultimate strength divided by tensile strength of NFM is in proportional relation with Young's modulus as shown in Fig. 8. The foregoing relation is used in Eq. (4.1) and Eq. (4.2) to calculate the friction restraint by TCR of NFM.

4.1 Maximum strength

Shear capacity Q_{ws} at flexural yielding of a united wall panel and shear strength Q_{vj} vertical joint are shown as follows. Shear strengths at shear failure of a united wall panel and at shear failure of horizontal joint, Q_{ws} , Q_{vj} respectively are independent to failure in this test and shear capacity Q_{ws} at flexural yielding of a united wall panel is calculated by the conventional equation, therefore equations of these values are omitted.

$$Q_{vj} = (Q'_{vj} + Q_{ws}) \cdot (L/H) \quad \dots (4.1)$$

where,

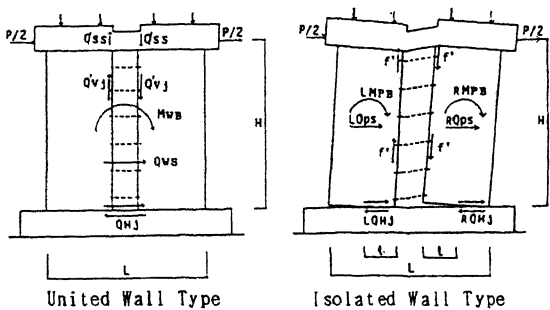


Fig. 7 Model of Resistant Mechanism

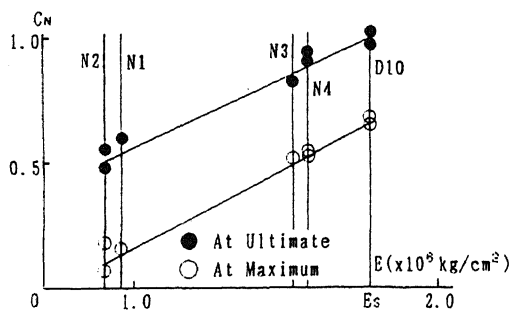


Fig. 8 Relation between Young's Modulus and Effect Ratio of TCR

$$Q'_{vj} = 0.09F_{vc}A_c + 1.48a_c\sqrt{\sigma_y F_{vc} + \mu C_c a_c \sigma_{cy}} + \mu C_b \frac{E_N - 0.688 \times 10^6}{E_S - 0.688 \times 10^6} a_b \sigma_{by} \dots (4.1a)$$

$$Q_{ss} = \left(\frac{0.0679 \times p_t^{0.23} (F_c + 180)}{\sqrt{a/d + 0.12}} + 0.1 \sigma_o \right) b_j \dots (4.1b)$$

- a: shear span distance of TCP
- A_c: total area of cotter
- a_b(a_c): total area of TCR (cotter reinforcement)
- b: width of TCP
- C_b=0.5 (C_c=0.64): coefficient of reduction of TCR (cotter reinforcement) at maximum strength
- d: effective depth of TCP
- E_S(E_N): Young's modulus of reinforcement (CFRP)
- F_c: compressive strength of concrete
- F_{vc}: compressive strength of joint concrete
- p_t: ratio of tensile reinforcement of stub
- σ_{cy}: (σ_{cy}): tensile strength of TCR (cotter reinforcement)
- σ_o: axial stress of stub
- σ_y: yield stress of reinforcement
- μ=0.84: coefficient of friction

4.2 Ultimate strength

Shear capacity Q_{PB} of flexural yielding of wall panel are shown as follows. Shear strength Q_{HJ} of horizontal joint is independent to failure, therefore equation of that value is omitted.

$$Q_{PB} = LQ_{PB} + RQ_{PB} \dots (4.2)$$

where,

$$LQ_{PB} = (LM_{PB} + lf')/H \quad RQ_{PB} = (RM_{PB} + lf')/H \quad (4.2a)$$

$$f' = \mu (C_c a_c \sigma_{cy} + C_b \frac{E_N - 0.688 \times 10^6}{E_S - 0.688 \times 10^6} a_b \sigma_{by}) \dots (4.2b)$$

C_b(C_c)=1.0; coefficient of reduction of TCR (cotter reinforcement) at ultimate strength
 f': friction force by cotter and TCR
 l: distance between longitudinal center of isolated wall panel and interface of vertical joint

Table 4 shows the comparison of calculated results and experimental ones. From Table 4 it is shown that calculated values comparatively agree with experimental ones. Therefore, equation of shear strength obtained by S-type shear experiment by the author may be said to be applicable to predict the shear capacity of wall panel.

Table 4 Calculated Strengths

Specimen	Calculated Values (tf)					
	Flexural Strength of Wall Panel	Maximum Strength at Vertical Joint			Ultimate Flexural Strength of Wall Panel	Ultimate Flexural Strength of Isolated Wall Panel
		Strength of Joint	Strength of TCP	Total		
WPC-N2	27.85	26.04	2.31	25.68	—	20.85
WPC-N4	27.85	30.08	3.23	30.17	27.85	—
Experimental Values (tf)						
Specimen	Maximum Strength			Ultimate Strength		
	Exp.	Exp./Cal.	Exp./Cal.	Exp.	Exp./Cal.	
WPC-N2	26.48	1.03	20.30	0.98	—	
WPC-N4	28.86	1.04	28.86	1.04	—	

5. Conclusions

- Conclusions are as follows.
- 1) Shear strength equations obtained from the S-type test are applicable to the prediction of the strength of the cantilever-type wall panel.
- 2) Both rigidity and strength of the TCR have great effect to opening and sliding deformation at vertical joint and failure mode of wall panel structures.
- 3) The maximum and the ultimate strength of wall panel structures are predicted using the shear strength equation of vertical joint presented by the author.
- 4) The failure mode of wall panel structures may be anticipated controlling the combination of tensile rigidity and strength of TCR using the new material such as CFRP.

REFERENCES

[1]Tayama, K., Mochizuki, S., Nishioka, T., & Fujisaki, T. 1990 Experiment on vertical joint using FRP reinforcement of wall panel precast concrete structures. *Proc. of ACI* :12-1 pp.1061~1064

[2]Mochizuki, S., 1990. Shear behaviors of vertical joint of wall panel structure. *Transaction of AIJ* :Vol. 413, pp.11~22